IEEE Photonics Journal
An IEEE Photonics Society Publication

Freeform Lens Design of Beam Shaping With User-Defined Rotation-Symmetric Profile by Using Numerical Method

Volume 11, Number 3, June 2019

Cheng-Mu Tsai
Chen-Kang Wu

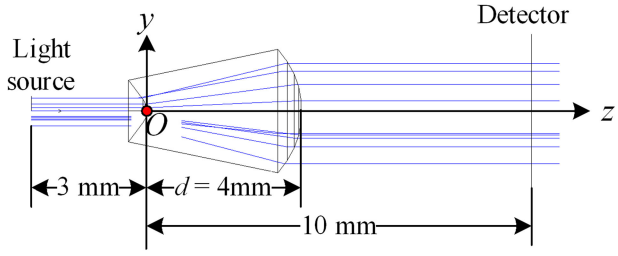

DOI: 10.1109/JPHOT.2019.2916587
1943-0655

Freeform Lens Design of Beam Shaping With User-Defined Rotation-Symmetric Profile by Using Numerical Method

Cheng-Mu Tsai and Chen-Kang Wu

Graduate Institute of Precision Engineering, National Chung Hsing University, Taichung City 402, Taiwan, R.O.C.

DOI:10.1109/JPHOT.2019.2916587

Manuscript received April 29, 2019; accepted May 9, 2019. Date of publication May 16, 2019; date of current version May 20, 2019. This work was supported in part by the Ministry of Science and Technology of Taiwan under Contract MOST 107-2221-E-005-050, and in part by the National Chung Hsing University, Taiwan, R.O.C. Corresponding author: Cheng-Mu Tsai (e-mail: jmutsai@email.nchu.edu.tw).

Abstract: A freeform lens construction is proposed to form a specific rotation symmetric beam profile with collimation in this paper. In the proposed approach, two freeform surfaces are constructed segment-by-segment using a numerical method based on Snell's law to produce an output beam profile which has both good irradiance uniformity and high collimation. It is shown that as the number of segments used to construct the freeform surfaces increases, the output beam profile approaches the specific profile. A sparse design point freeform surface construction method is additionally proposed which allows the beam profile to approach the desirable distribution with a fewer number of segments. The proposed method is used to construct freeform lenses for producing output beams with two user-defined irradiance patterns, i.e., annular and triangular distributions. The simulation results show that either demonstrated irradiance distribution is close to the specific distribution. Overall, the present results show that the proposed method provides a versatile and efficient approach for designing freeform lenses with a specific distribution of the output beam profile and good collimation.

Index Terms: Beam shaping, uniformity, collimation.

1. Introduction

A beam shaping finds extensive use nowadays for a wide range of applications. In most cases, the Gaussian profile of the beam must be reshaped to a more desirable distribution (e.g., uniformity) prior to use [1]–[11]. Cao *et al.* [7] developed a center off-axis microlen array system for generating a far-field irradiance distribution with good homogeneity. However, in many beam forming applications, it is necessary to produce an output beam which has not only good irradiance uniformity, but also high collimation. In practice, this requires the use of at least two lens surfaces, namely one surface to achieve uniformity and a second surface to achieve collimation.

Many beam shaping systems have been proposed for constructing beam profiles with uniformity and collimation [1]–[6], [9], [10]. For example, Frieden [1] presented a beam shaping system in which the original Gaussian profile of the beam was transformed into collimated uniform irradiance with power lossless. However, the uniformity produced at the second surface is easily broken by the third surface since the structures of the two surfaces are related to each other. Rhodes and Shealy

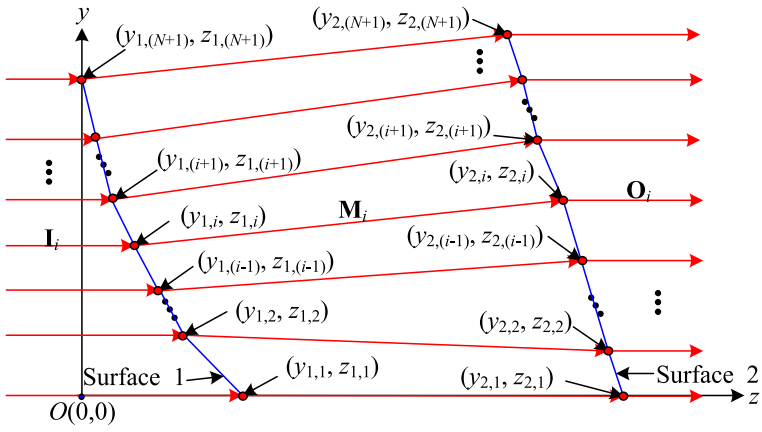

Fig. 1. Freeform lens design method for achieving uniformity and collimation simultaneously.

[2] recognized this problem and developed a refractive optical system for achieving the uniform irradiance with collimated radiation. However, some applications require a collimated output beam, but a non-uniform distribution of the irradiance. Developing optical systems capable of meeting this requirement deducing an analytic solution represents a significant challenge, especially for a non-collimated light source. Thus, the use of numerical methods [10] to construct freeform lenses [12], [13] has attracted growing interest in recent decades.

The present study proposes a numerical method for constructing a freeform lens for producing an output beam with both high collimation and a user-defined irradiance pattern. In the proposed approach, the first surface is designed to achieve the user-specified irradiance distribution, while the second surface is designed to both maintain the required irradiance distribution and achieve high collimation. Both surfaces are constructed using a segment-by-segment approach based on Snell's law. It is shown that the irradiance uniformity of the constructed freeform lens is in good agreement with given the use of sufficient ($N = 4000$) segments to construct the lens surfaces. Alternative construction method is proposed based on a sparse number of design points to construct freeform lenses which approach the desirable profile for the output irradiance with a lower number of segments ($N = 2000$). The validity of the proposed method is demonstrated by constructing freeform lenses for producing output beams with two user-defined irradiance patterns, that is, annular and triangular distributions. The simulation results show that either intensity distribution produced by the designed lenses approaches the specific profile.

The remainder of this paper is organized as follows. Section 2 describes the proposed fundamental freeform lens construction method. Section 3 presents the simplified freeform lens construction method based on a sparse number of design points. Section 4 illustrates how to make the irradiance with the user-defined pattern and demonstrates the feasibility of the proposed method for designing freeform lenses with annular and triangular output irradiance patterns, respectively. Finally, Section 5 provides some brief concluding remarks and indicates the intended direction of future research.

2. Fundamental Freeform Lens Design Method for Producing Output Irradiance With Good Uniformity and Collimation

The aim of beam shaping is to modify an input beam with a known irradiance distribution into an output beam with a certain user-defined power profile. Most applications require the output irradiance to be both uniformly distributed and collimated. As shown in Figure 1, this is generally achieved using a minimum of two surfaces. The task of the first surface is to ensure a uniform distribution of the beam irradiance, while that of the second surface is to maintain the irradiance

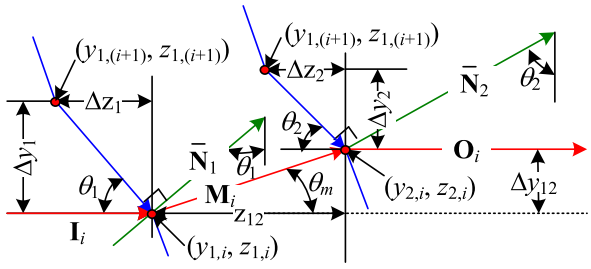

Fig. 2. Sag determination of two freeform surfaces.

uniformity and achieve high collimation. Note that the aim of the first surface is to achieve irradiance uniformity on the second (curved) surface rather than on a flat plane [2]. In other words, the construction of the two surfaces must proceed jointly rather than independently.

In developing the design method proposed in this study, it is assumed that the light source has a collimated rotation-symmetric profile. It is further assumed that the surfaces of the freeform lens consist of N segments, where each segment receives the same power. As shown in Fig. 1, the heights of the design points used to define these segments on Surface 1 are denoted as $(y_{1,1}, y_{1,2}, \ldots, y_{1,N+1})$. Similarly, the heights of the design points on Surface 2 are denoted as $(y_{2,1}, y_{2,2}, \ldots, y_{2,N+1})$ that are required to be the same area for the uniformity, that is, $y_{2,i} = [(i-1)R_2^2/N]^{1/2}$ for $i = 1, \ldots, N$, where R_2 is the spot radius of the beam at the output. To achieve a uniform irradiance distribution, the rays incident in the y-direction at heights $(y_{1,1}, y_{1,2}, \ldots, y_{1,N+1})$ on Surface 1 must be re-directed such that they are incident at heights $(y_{2,1}, y_{2,2}, \ldots, y_{2,N+1})$ on Surface 2. Without loss of generality, the light source with a rotation-symmetric profile in Fig. 1 can be assumed to have a Gaussian distribution, i.e.,

$$I(y) = I_0 e^{-2\left(\frac{y}{\sigma}\right)^2} \tag{1}$$

where I_0 is the power at the center of the beam, y is the radial distance from the center of the beam, and σ is the variance. As described above, the power of the light source incident on Surface 1 is partitioned equally into N parts, that is,

$$\begin{aligned} P_{1,i} &= \int_0^{2\pi} \int_{y_{1,i}}^{y_{1,(i+1)}} I_0 e^{-2\left(\frac{y}{\sigma}\right)^2} y\,dy\,d\phi \\ &= 2\pi \int_{y_{1,i}}^{y_{1,(i+1)}} I_0 e^{-2\left(\frac{y}{\sigma}\right)^2} y\,dy \qquad \text{for} = 1, 2, \ldots, N \\ &= \frac{2\pi \int_0^{R_1} I_0 e^{-2\left(\frac{y}{\sigma}\right)^2} dy}{N} = \text{const} \end{aligned} \tag{2}$$

where R_1 is the radius of the light source beam, $y_{1,1} = 0$ (i.e., the optical axis), and height position $y_{1,(i+1)}$ can be found using suitable software (e.g., Matlab). In solving the lens design problem, it is required that the ray incident on Surface 1 at point $y_{1,(i+1)}$ is refracted such that it strikes Surface 2 at point $y_{2,(i+1)}$ and hence ensures uniformity, as shown in Figure 1.

Figure 2 presents a schematic illustration of the method proposed in this study for constructing two freeform surfaces capable of generating a collimated rotation-symmetric output beam with a normal uniform irradiance distribution. Consider two points $(y_{1,i}, z_{1,i})$ and $(y_{2,i}, z_{2,i})$ on Surfaces 1 and 2, respectively. The vector of the refractive ray between them can be expressed as

$$\mathbf{M}_i = \frac{[0\ \Delta y_{12}\ z_{12}]}{\sqrt{\Delta y_{12}{}^2 + z_{12}{}^2}} \tag{3}$$

where $\Delta y_{12} = (y_{2,i} - y_{1,i})$ and $z_{12} = (z_{2,i} - z_{1,i})$. The normal line $\mathbf{N}_1 = [0, n_{1,1}, n_{1,2}]$ for the i-th segment of Surface 1 can be determined from Snell's as [12]

$$\left[1 + {n_r}^2 - -2n_r\left(\mathbf{M}_i \cdot \mathbf{I}_i\right)\right]^{1/2}\mathbf{N}_1 = \mathbf{M}_i - -n_r\mathbf{I}_i \tag{4}$$

where $n_r = 1/n$ and n is the refractive index of the freeform lens material. In addition, $\mathbf{I}_i$ is the unit vector of the i-th segment and is defined with respect to the incident ray in collimation, i.e., $\mathbf{I}_i = [0\,0\,1]$. From basic geometric principles, the distance Δz_1 between $z_{1,(i+1)}$ and $z_{1,i}$ is given by

$$\Delta z_1 = \Delta y_1 \cot(\theta_1) = \Delta y_1 \frac{n_{1,1}}{n_{1,2}} \tag{5}$$

where $\Delta y_1 = y_{1,(i+1)} - y_{1,i}$. Since the heights of the design points on Surface 1, i.e., $(y_{1,1}, y_{1,2}, \ldots, y_{1,N+1})$, have previously been calculated in solving Eq. (2), the z-position of the next point $(y_{1,i+1}, z_{1,(i+1)})$ on Surface 1 can be found as

$$z_{1,(i+1)} = z_{1,i} - \Delta z_1 \tag{6}$$

The incident ray passing through point $(y_{1,i}, z_{1,i})$ on Surface 1 should be refracted through the plane created by points $(y_{1,i}, z_{1,i})$ and $(y_{1,i+1}, z_{1,i+1})$ such that it is directed to point $(y_{2,i}, z_{2,i})$ on Surface 2, and hence achieves uniformity.

Having ensured uniformity at Surface 2, it is necessary to construct Surface 2 such that the output rays not only retain uniformity, but are also collimated. In solving this problem, $z_{2,(i+1)}$ is unknown. As for the previous task of determining point $z_{1,(i+1)}$ on Surface 1, Snell's law can be applied to find the normal line $\mathbf{N}_2 = [0, n_{2,1}, n_{2,2}]$ at point $(y_{2,i}, z_{2,i})$ on Surface 2, that is,

$$\left[1 + n^2 - -2n\left(\mathbf{O}_i \cdot \mathbf{M}_i\right)\right]^{1/2}\mathbf{N}_2 = \mathbf{O}_i - -n\mathbf{M}_i \tag{7}$$

where $\mathbf{O}_i$ is the unit vector of the i-th segment of Surface 2 and is defined with respect to the output ray in collimation, i.e., $\mathbf{O}_i = [0\,0\,1]$. The distance Δz_2 between points $z_{2,(i+1)}$ and $z_{2,i}$ can be obtained geometrically as

$$\Delta z_2 = \Delta y_2 \cot(\theta_2) = \Delta y_2 \frac{n_{2,1}}{n_{2,2}} \tag{8}$$

where $\Delta y_2 = y_{2,(i+1)} - y_{2,i}$. As described above, the heights of the design points on Surface 2, i.e., $(y_{2,1}, y_{2,2}, \ldots, y_{2,N+1})$, are arranged in such a way that each segment receives an equal power in the same height. Consequently, the next point $(y_{2,i+1}, z_{2,(i+1)})$ in the z direction of Surface 2 is given as

$$z_{2,(i+1)} = z_{2,i} - \Delta z_2 \tag{9}$$

Creating a plane between points $(y_{2,i}, z_{2,i})$ and $(y_{2,i+1}, z_{2,(i+1)})$ ensures that the rays are collimated through Surface 2. Given initial points $(y_{1,1}, z_{1,1}) = (0,0)$ and $(y_{2,1}, z_{2,1}) = (0, d)$, Surfaces 1 and 2 can be constructed numerically using Eqs. (2)–(9) to create a freeform lens which ensures that the output light is both uniform and collimated. Note that d is the distance between the apexes of the two freeform surfaces.

The validity of the design method described above was demonstrated using a light source with a collimated Gaussian profile, a beam radius of 0.8 mm, and an operating wavelength of 0.633 μm. In designing the lens, the aim was to expand the spot radius of the beam to 1.6 mm. The lens was assumed to be fabricated of POLYCARB. Furthermore, the lens thickness was specified as $d = 4$ mm. Figure 3 presents a schematic illustration of the considered design problem, where the number of surface segments was set as $N = 5$ for simplicity purposes. The coordinates of the designed points on Surfaces 1 and 2 are listed in Table 1. The optical performance of the lens was evaluated by means of Zemax simulations under the assumption of a light source with a power of 5 mW located at a distance of 3 mm in front of Surface 1. The simulations traced a total of 10 million rays. As shown in Fig. 3, a detector was placed 10 mm behind Surface 1 to receive the traced rays.

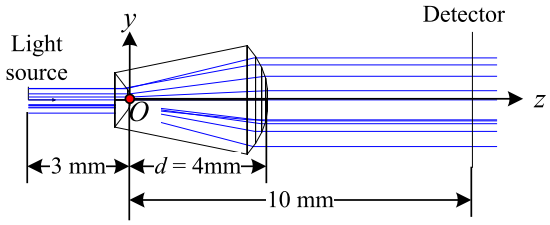

Fig. 3. Freeform lens design for simple case of $N = 5$.

TABLE 1
Point Coordinates of Freeform Lens for $N = 5$

Pair #	1	2	3	4	5	6
Surface	(0, 0)	(0.156,0.000)	(0.236,-0.031)	(0.316,-0.076)	(0.419,-0.146)	(0.800,-0.443)
Surface	(0.000,4.000)	(0.716,4.000)	(1.012,3.885)	(1.239,3.759)	(1.431,3.627)	(1.600,3.495)

The detector had a size of 250 × 250 pixels and was used to detect the irradiance pattern over the range of −2 mm to 2 mm and the collimation of the output rays over the range of −0.1° to 0.1°.

Figure 4 shows the simulation results. It is seen in Figs. 4(a) and 4(b) that the designed lens fails to achieve the required uniform distribution of the output irradiance. In particular, a high irradiance peak is observed in the central region of the detection plane. This result is due most likely to the small number of segments ($N = 5$) used to construct the freeform surfaces. However, the shaped beam has excellent collimation (i.e., less than 0.02°), as shown in Fig. 4(c). Figure 5(a) shows the uniformity distributions obtained when constructing the freeform surfaces using $N = 1000$, 2000 and 4000 segments, respectively. As expected, the uniformity improves significantly with increasing N due to the greater smoothness of the lens surfaces. Irrespective of the value of N, the collimation remains lower than 0.05°, as shown in Fig. 5(b).

3. Alternative Freeform Surface Construction Method Based on Sparse Design Points Method

This section presents an alternative surface construction method which enables the uniformity of the irradiance distribution to approach the desirable profile using fewer surface segments than that required in the original method. Figure 6 presents a schematic illustration of the proposed approach. As described in Section 2, the heights of the original design points on Surfaces 1 and 2 are denoted as ($y_{1,1}$, $y_{1,2}$, …, $y_{1,N+1}$) and ($y_{2,1}$, $y_{2,2}$, …, $y_{2,N+1}$), respectively, and are determined from the same procedures of the original method. In the proposed method, referred to hereafter as the sparse design points method, the two freeform surfaces are constructed using a new set of design points located at the mid-point positions between the original points. Since the surfaces are constructed based on the middle of the original heights, it is anticipated that such an approach can maintain the uniformity of the irradiance distribution on Surface 2 while simultaneously reducing the number of design points which must be processed. As shown in Fig. 6, the new set of design points are thus specified as

$$ym_{s,i} = \left(y_{s,i-1} + y_{s,i}\right)/2 \,\text{for}\, i = 2, \ldots, N+1 \tag{10}$$

where s is 1 or 2 (for Surface 1 or Surface 2, respectively), and $ym_{s,1} = y_{s,1}$ and $ym_{s,N+2} = y_{s,N+1}$.

Once the heights ($ym_{1,1}$, $ym_{1,2}$, …, $ym_{1,N+2}$) and ($ym_{2,1}$, $ym_{2,2}$, …, $ym_{2,N+2}$) of the design points on Surfaces 1 and 2, respectively, have been determined from Eq. (10), it is necessary to establish the points ($zm_{1,1}$, $zm_{1,2}$, …, $zm_{1,N+2}$) and ($zm_{2,1}$, $zm_{2,2}$, …, $zm_{2,N+2}$) on the two

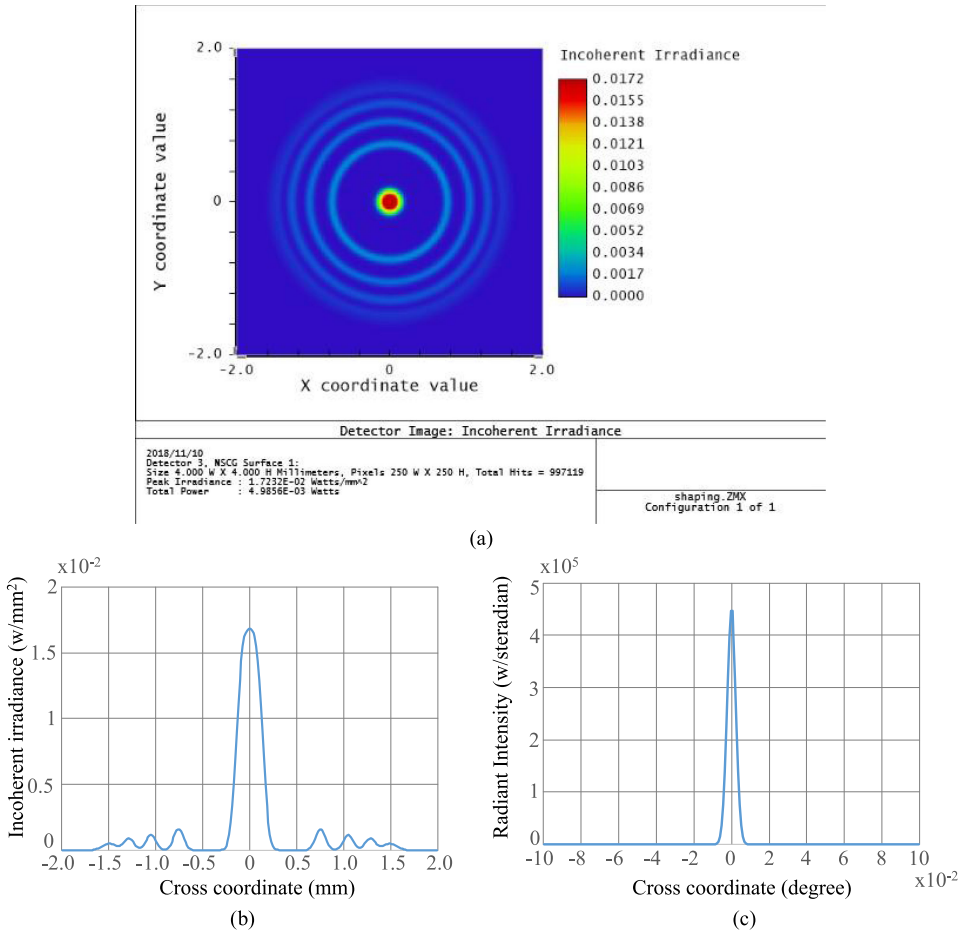

Fig. 4. Simulation results for freeform lens given $N = 5$. (a) spot irradiance. (b) Cross-section of spot irradiance. (c) Cross-section of radiance intensity.

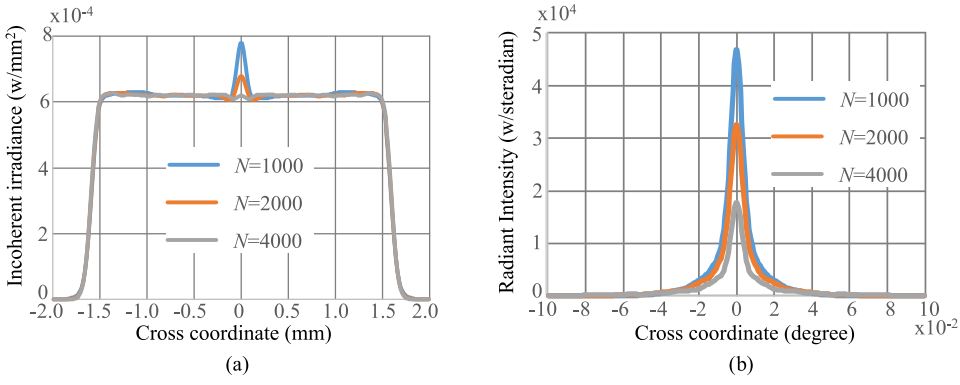

Fig. 5. Simulation results obtained for different values of *N*. (a) Cross-section of spot irradiance. (b) Cross-section of radiance intensity.

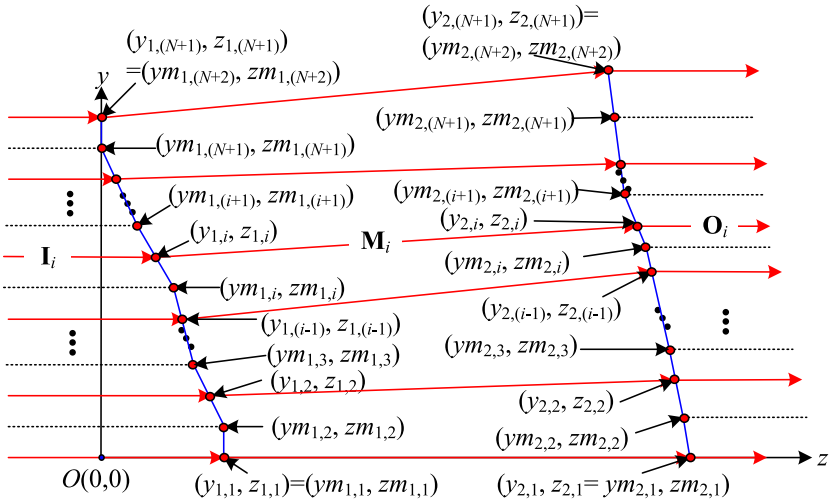

Fig. 6. Freeform lens design method based on sparse design points.

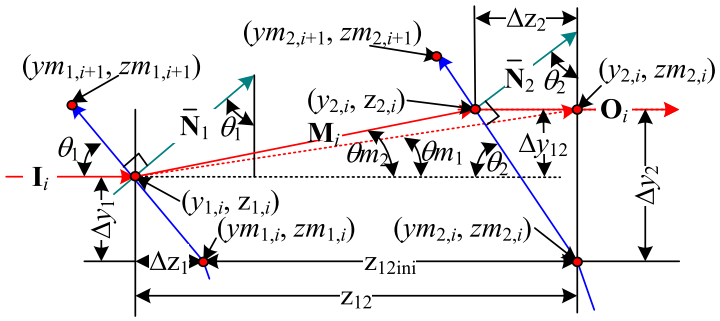

Fig. 7. Sag determination using sparse design points method.

surfaces which ensure both uniformity and collimation. Given points $(ym_{1,i},\ zm_{1,i})$ and $(y_{2,i},\ zm_{2,i})$ in Fig. 7, and heights $y_{1,i}$ and $y_{2,i}$, it can be shown that

$$\sin\theta_1 = \frac{\Delta y_1}{\sqrt{(\Delta z_1{}^2 + \Delta y_1{}^2)}} \tag{11a}$$

$$\cos\theta_1 = \frac{\Delta z_1}{\sqrt{(\Delta z_1{}^2 + \Delta y_1{}^2)}} \tag{11b}$$

$$\sin\theta m_1 = \frac{\Delta y_{12}}{\sqrt{[(z_{12ini} + \Delta z_1)^2 + \Delta y_{12}{}^2]}} \tag{11c}$$

$$\cos\theta m_1 = \frac{(z_{12ini} + \Delta z_1)}{\sqrt{[(z_{12ini} + \Delta z_1)^2 + \Delta y_{12}{}^2]}} \tag{11d}$$

where $\Delta y_1 = (y_{1,i} - ym_{1,i})$, $\Delta y_{12} = (y_{2,i} - y_{1,i})$, and $z_{12ini} = (zm_{2,i} - zm_{1,i})$. The normal vector of Surface 1 is given as $\mathbf{N}_1 = [0\ \cos\theta_1\ \sin\theta_1]$, while the input vector is given as $\mathbf{I} = [0\ 0\ 1]$. Moreover, the vector of the refractive ray between points $(y_{1,i},\ z_{1,i})$ and $(y_{2,i},\ zm_{2,i})$ has the form $\mathbf{M}_i = [0\ \sin\theta m_1\ \cos\theta m_1]$. Applying Snell's law in Eq. (4), and performing algebraic manipulation, the

following fourth-order polynomial in Δz_1 can be obtained:

$$(1-{n_r}^2)\Delta {z_1}^4 + 2(1-{n_r}^2)z_{12ini}\Delta {z_1}^3 + [-2\Delta y_1 \Delta y_{12} + (1-{n_r}^2){z_{12ini}}^2 - {n_r}^2{\Delta y_{12}}^2]\Delta {z_1}^2 - 2\Delta y_1 \Delta y_{12} z_{12ini}\Delta z_1 + {\Delta y_1}^2{\Delta y_{12}}^2 = 0 \quad (12)$$

Having determined Δz_1, the normal vector $\mathbf{N}_1 = [0\ \cos\theta_1\ \sin\theta_1]$ can be obtained from Eqs. (11a) and (11b). From Fig. 7, $z_{1,i}$ and $zm_{1,i+1}$ are represented by

$$z_{1,i} = zm_{1,i} - \Delta y_1 \frac{\cos\theta_1}{\sin\theta_1} \quad (13a)$$

$$zm_{1,(i+1)} = zm_{1,i} - [ym_{1,(i+1)} - ym_{1,i}]\frac{\cos\theta_1}{\sin\theta_1} \quad (13b)$$

Δz_2 can be obtained using the same procedure as that for Δz_1; but with regard to points $(y_{1,i},\ z_{1,i})$ and $(ym_{2,i},\ zm_{2,i})$ rather than $(ym_{1,i},\ zm_{1,i})$ and $(y_{2,i},\ zm_{2,i})$, respectively. From basic geometric principles, it is easily shown that

$$\sin\theta_2 = \frac{\Delta y_2}{\sqrt{(\Delta {z_2}^2 + \Delta {y_2}^2)}} \quad (14a)$$

$$\cos\theta_2 = \frac{\Delta z_2}{\sqrt{(\Delta {z_2}^2 + \Delta {y_2}^2)}} \quad (14b)$$

$$\sin\theta m_2 = \frac{\Delta y_{12}}{\sqrt{[(z_{12} - \Delta z_2)^2 + {\Delta y_{12}}^2]}} \quad (14c)$$

$$\cos\theta m_2 = \frac{(z_{12} - \Delta z_2)}{\sqrt{[(z_{12} - \Delta z_2)^2 + {\Delta y_{12}}^2]}} \quad (14d)$$

where $\Delta y_2 = (y_{2,i} - ym_{2,i})$ and $z_{12} = (zm_{2,i} - z_{1,i})$. The normal vector $\mathbf{N}_2$ has the form $[0\ \cos\theta_2\ \sin\theta_2]$. Meanwhile, the vector of the refractive ray between points $(y_{1,i},\ z_{1,i})$ and $(y_{2,i},\ z_{2,i})$ is given as $\mathbf{M}_i = 0\sin\theta m_2\cos\theta m_2]$ and the output vector $\mathbf{O}_i$ is $[0\ 0\ 1]$. The following polynomial expression is finally obtained:

$$(n^2-1)\Delta {z_2}^4 - 2(n^2-1)z_{12}\Delta {z_2}^3 + [2n^2\Delta y_{12}\Delta y_2 + (n^2-1){z_{12}}^2 - {\Delta y_{12}}^2]\Delta {z_2}^2 - 2n^2\Delta y_{12}\Delta y_2 z_{12}\Delta z_2 + n^2{\Delta y_{12}}^2{\Delta y_2}^2 = 0 \quad (15)$$

An appropriate solution for Δz_2 can be found using software such as Matlab. Points $z_{2,i}$ and $zm_{2,i+1}$ can then be obtained as

$$z_{2,i} = zm_{2,i} - \Delta y_2 \frac{\cos\theta_2}{\sin\theta_2} \quad (16a)$$

$$zm_{2,(i+1)} = zm_{2,i} - [ym_{2,(i+1)} - ym_{2,i}]\frac{\cos\theta_2}{\sin\theta_2} \quad (16b)$$

All of the points $(zm_{1,1},\ zm_{1,2},\ \ldots,\ zm_{1,N+2})$ and $(zm_{2,1},\ zm_{2,2},\ \ldots,\ zm_{2,N+2})$ on Surfaces 1 and 2 can be similarly obtained using Eqs. (11)–(16). Figure 8 compares the simulation results obtained from the sparse design points method for the uniformity (Fig. 8(a)) and collimation (Fig. 8(b)) for the design problem shown above in Fig. 3. Note that $N = 1000$ and $N = 2000$ in alternative freeform surface construction cases. For comparison purposes, the solution obtained using the original method with $N = 4000$ segments is also presented. It is seen that the uniformity obtained using the proposed sparse design points method approaches that of the ideal case despite the use of fewer design points than the original method (i.e., $N = 4000$). Furthermore, the collimation performance of the original method (i.e., $<0.05^\circ$) is maintained.

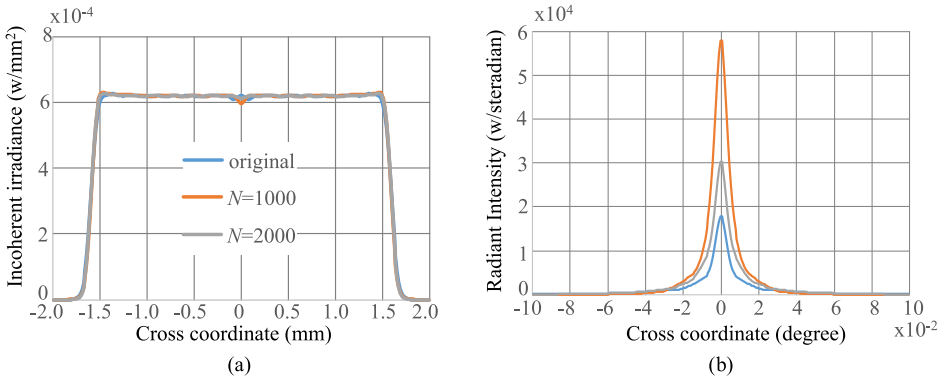

Fig. 8. Simulation results obtained using sparse design points method. (a) Cross-section of spot irradiance. (b) Cross-section of radiance intensity.

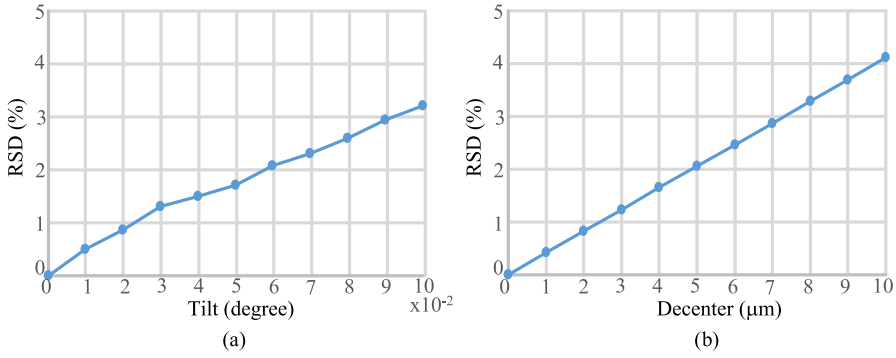

Fig. 9. Tolerance analysis for (a) tilt, and (b) decenter.

A tolerance analysis with tilt and decenter is estimated for the proposed freeform lens, as shown in Figure 9. The relative standard deviation (RSD) [14] is applied to analyze the tolerance, which is expressed as

$$RSD = \sqrt{\frac{1}{N_P}\sum_{i=1}^{N_P}\left[\frac{I_T(i) - I_0(i)}{I_0(i)}\right]^2} \tag{17}$$

where N_P is the number of the major contributed points, $I_T(i)$ is the simulated illuminance with tolerance at the i-th major contributed point and $I_0(i)$ is the illuminance at the i-th major contributed point without tilt and decenter. Figure 9(a) shows that there is 0.1° tolerance for the freeform tilt under the RSD 5% requirement. The decenter of the freeform allows at least 10 μm tolerance for the RSD 5% requirement, as shown in Figure 9(b). The collimation keeps less than 0.2° for all the tilt and decenter under 0.1° and 10 μm, respectively. There are many fabrication processes for the lens design [15]–[17]. Kumler and Buss [16] proposed micron-level alignment to allow 0.5 μm alignment accuracy. Wenzel *et al.* [17] applied a machine program for an untrue turning process to calculate data in a fully automated manner, which permitting the tilt and decenter around 0.06 arcmin and 0.63 mm, respectively. It is easy to promise the tolerance with tilt and decenter under 0.1° and 10 μm. As a result, the current fabrication process can satisfy the precision requirement for building the proposed beam shaping freeform lens.

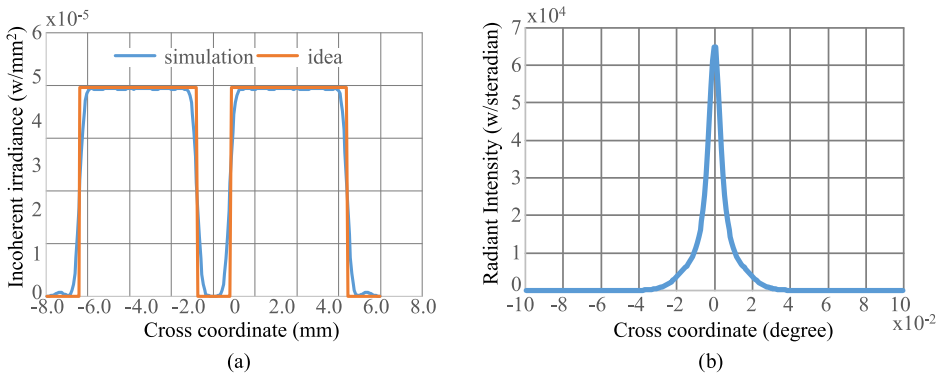

Fig. 10. Simulation results obtained for annular irradiance profile using sparse design points method with $N = 1000$. (a) Cross-section of spot irradiance. (b) Cross-section of radiance intensity.

4. Beam Shaping With Collimated Rotation-Symmetric Profile Using User-Defined Irradiance Pattern

In traditional beam shaping methods, it is necessary to produce an output beam with good irradiance uniformity and high collimation. However, in some applications, it is desirable to produce an output beam which retains good collimation, but has a certain user-defined irradiance profile instead. As described in Sections 2 and 3, in traditional beam forming, the heights of the design points on Surface 2 are assigned in such a way as to achieve a uniform irradiance distribution. By contrast, to obtain a specific (non-uniform) rotation-symmetric profile of the output light, the heights of the design points should be arranged according to a certain irradiance distribution $I_{output}(y)$, i.e.,

$$\begin{aligned} P_{2,i} &= \int_0^{2\pi} \int_{y_{2,i}}^{y_{2,(i+1)}} I_{output}(y) y \, dy \, d\phi \\ &= 2\pi \int_{y_{2,i}}^{y_{2,(i+1)}} I_{output}(y) y \, dy \qquad \text{for } i = 1, 2, \ldots, N \\ &= \frac{2\pi \int_0^{R_2} I_{output}(y) y \, dy}{N} = \text{const} \end{aligned} \tag{18}$$

where R_2 is the radius of the output beam and $y_{2,1}$ is the height of the initial design point on Surface 2. As before, the height of point $y_{2,(i+1)}$ can be obtained using software such as Matlab.

For illustration purposes, consider the case where the output beam is required to have an annular profile. In other words,

$$I_{output}(y) = \begin{cases} 3.95 \cdot 10^{-5} & \text{for } 0.8 < y < 6.4 \\ 0 & \text{otherwise} \end{cases} \tag{19}$$

The corresponding simulation results are shown in Fig. 10. Note that, the freeform lens was constructed using the sparse design points method described in Section 3 with $N = 1000$. Moreover, the thickness between the vertexes of Surfaces 1 and 2 was set as 15 mm. It is seen that the simulated irradiance profile in Fig. 10(a) is very close to the ideal annular distribution. Furthermore, the collimation has a value of less than 0.05°, as shown in Fig. 10(b).

Consider the following further example, in which the output irradiance is required to have a triangular distribution, i.e.,

$$I_{output}(y) = \begin{cases} c \cdot (6.4 - y) & \text{for } 0.8 < y < 6.4 \\ 0 & \text{otherwise} \end{cases} \tag{20}$$

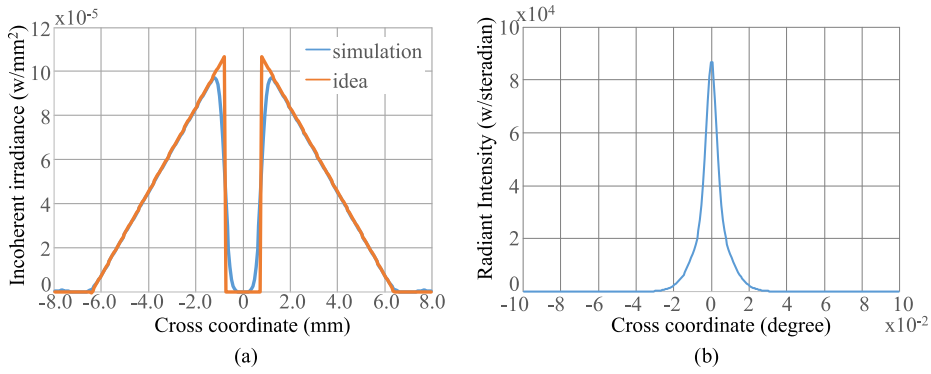

Fig. 11. Simulation results obtained for triangular irradiance profile using sparse design points method and $N = 1000$. (a) Cross-section of spot irradiance. (b) Cross-section of radiance.

where c is a constant that depends on the overall power of the illumination source. Figure 11(a) shows the simulation results obtained when using Eq. (20) with $c = 1.07 \times 10^{-4}$ and an overall power of 5 mW. The results confirm that the simulated irradiance profile approaches the required distribution, as shown in Fig 11.

5. Conclusions and Future Work

A numerical beam shaping method has been proposed for constructing freeform lenses capable of producing an output beam with both a uniform irradiance distribution and good collimation. In the proposed approach, the two surfaces of the freeform lens are constructed segment-by-segment based on Snell's law. The simulation results have shown that the irradiance distribution and collimation approach the ideal case given a sufficiently large number of segments ($N = 4000$). The proposed method, designated as the sparse design points method, has been used to construct two freeform lenses for producing output beams with annular and triangular irradiance distributions, respectively. The simulation results have shown that either irradiance profile produced by the designed lenses is close to the user-defined profile. Moreover, the lens achieves a collimation of less than 0.05°. As a result, the proposal is flexible way to deduce the freeform lens to make the beam shaping with specific collimated rotation symmetrical distribution. Since the proposal is based on the collimated light source, the future work is to design a freeform lens to convert a light source with divergence and astigmatism attribution like a semiconductor laser into a circular collimation and uniformity output.

Acknowledgment

The authors would like to thank the anonymous reviewers for their valuable suggestions.

References

[1] B. R. Frieden, "Lossless conversion of a plane laser wave to a plane wave of uniform irradiance," *Appl. Opt.*, vol. 4, no. 11, 1965, pp. 1400–1403, 1965.
[2] P. W. Rhodes and D. L. Shealy, "Refractive optical systems for irradiance redistribution of collimated radiation: Their design and analysis," *Appl. Opt.*, vol. 19, no. 20, pp. 3545–3553, 1980.
[3] S. Zhang, G. Neil, and M. Shinn, "Single-element laser beam shaper for uniform flat-top profiles," *Opt. Exp.*, vol. 11, no. 16, pp. 1942–1948, 2003.
[4] C. Liu and S. Zhang, "Study of singular radius and surface boundary constraints in refractive beam shaper design," *Opt. Exp.*, vol. 16, no. 9, pp. 6675–6682, 2008.
[5] H. Ma, Z. Liu, P. Jiang, X. Xu, and S. Du, "Improvement of galilean refractive beam shaping system for accurately generating near-diffraction-limited flattop beam with arbitrary beam size," *Opt. Exp.*, vol. 19, no. 14, pp. 13105–13117, 2011.

[6] C. M. Tsai, Y. C. Fang, and C. T. Lin, "Application of genetic algorithm on optimization of laser beam shaping," *Opt. Exp.*, vol. 23, no. 12, pp. 15877–15887, 2015.
[7] A. X. Cao, H. Pang, J. Z. Wang, M. Zhang, L. F. Shi, and Q. L. Deng, "Center off-axis tandem microlens arrays for beam homogenization," *IEEE Photon. J.*, vol. 7, no. 3, Jun. 2015, Art. no. 2400207.
[8] D. Wang, B. Q. Jin, Y. Wang, P. Jia, D. M. Cai, and Y. Gao, "Adaptive flattop beam shaping with a spatial light modulator controlled by the holographic tandem method," *IEEE Photon. J.*, vol. 8, no. 1, Feb. 2016, Art. no. 6500107.
[9] C.-M. Tsai, "Uniformity and collimation of incoherence gaussian beam with divergence based on only one fresnel surface," *IEEE Photon. J.*, vol. 8, no. 6, Dec. 2016, Art. no. 6500509.
[10] C.-Y Tsai, "Refractive collimation beam shaper design and sensitivity analysis using a free-form profile construction method," *J. Opt. A, Pure Appl. Opt.*, vol. 34, no. 7, pp. 1236–1245, 2017.
[11] P. Han, H.-C Hsu, and C.-M Tsai, "Beam shaping freeform lens design with modified optical flux partition," *IEEE Photon. J.*, vol. 10, no. 1, Feb. 2018, Art. no. 8200113.
[12] K. Wang, S. Liu, F. Chen, Z. Qin, Z. Liu, and X. Luo, "Freeform LED lens for rectangularly prescribed illumination," *J. Opt. A, Pure Appl. Opt.*, vol. 11, no. 10, 2009, Art. no. 105501.
[13] C.-M Tsai and B.-X. Wang, "A freeform mirror design of uniform illumination in streetlight from a split light source," *IEEE Photon. J.*, vol. 10, no. 4, Aug. 2018, Art. no. 2201212.
[14] X. Mao, H. Li, Y. Han, and Y. Luo, "Polar-grids based source-target mapping construction method for designing freeform illumination system for a lighting target with arbitrary shape," *Opt. Exp.*, vol. 23, no. 4, pp. 4313–4328, 2015.
[15] K. Schwertz and J. Burge, *Field Guide to Optomechanical Design and Analysis*. Bellingham, WA, USA: SPIE Press, 2012.
[16] J. J. Kumler and C. Buss, "Sub-cell turning to accomplish micron-level alignment of precision assemblies," *Proc. SPIE*, vol. 10377, 2017, Art. no. 1037702.
[17] C. Wenzel *et al.*, "Advanced centering of mounted optics," *Proc. SPIE*, vol. 9730, 2016, Art. no. 973012.